Rend. Fis. Acc. Lincei (2016) 27 (Suppl 1):S173–S182
DOI 10.1007/s12210-016-0547-1



# A numerical algorithm for the assessment of the conjecture of a subglacial lake tested at Amundsenisen, Svalbard

**Daniela Mansutti[1] · Edoardo Bucchignani[2] · Piotr Glowacki[3]**

Received: 20 November 2015 / Accepted: 15 June 2016 / Published online: 30 June 2016
© Accademia Nazionale dei Lincei 2016

**Abstract** The melting of glaciers coming with climate change threatens the heritage of the last glaciation of Europe likely contained in subglacial lakes in Greenland and Svalbard. This aspect urges specialists to focus their studies (theoretical, numerical, and on-field) on such fascinating objects. Along this line, we have approached the validation of the conjecture of the existence of a subglacial lake beneath the Amundsenisen Plateau at South-Spitzbergen, Svalbard, where ground penetrating radar measurements have revealed several flat signal spots, the sign of the presence of a body of water. The whole investigation aspects, mathematical modeling and numerical simulation procedure, and the numerical results are presented through a trilogy of papers of which the present one is the last. The time-dependent mathematical model in the background of the numerical algorithm includes the description of dynamics and thermodynamics of the icefield and of the subglacial lake, with heat exchange and liquid/solid phase-change mechanisms at the interface. Critical modeling choices and confidence in the algorithm are granted by the numerical results of the sensitivity analysis versus the contribution of ice water content, of firn and snow layers at top of the icefield and versus the approximation of ice sliding on bedrock. The two previous papers deal with these issues, show successful comparison with local measured quantities, and demonstrate numerically the likelihood of the subglacial lake. In this work, we aim at providing the studied case and the numerical algorithm with a possible paradigmatic value. At this aim, we introduce on-field measurement data related to the physical characteristics of the Amundsenisen Plateau that justify the adoption of significant modeling simplifications, here, focussed from physical viewpoint. Furthermore, we present the numerical algorithm and discuss several representative results from the numerical test to point out the type of results coming from the procedure. Such results might, eventually, provide a support to the decision to undertake drilling operations for tracing the subglacial water biochemicals generally present within the accreted ice above the presumed ice/water front.

**Keywords** Temperate ice · Glen's law · Subglacial lake · Phase-change · Large Eddy Simulation · Svalbard · Finite volume

This peer-reviewed article is a result of the multi and interdisciplinary research activities based at the Arctic Station "Dirigibile Italia", coordinated by the "Dipartimento Scienze del Sistema Terra e Tecnologie per l'Ambiente" of the National Research Council of Italy.

✉ Daniela Mansutti
d.mansutti@iac.cnr.it

[1] Istituto per le Applicazioni del Calcolo "M. Picone" (CNR), Via dei Taurini, 19, 00186 Rome, Italy

[2] Centro Italiano Ricerche Aerospaziali, Via Maiorise, 1, 81043 Capua, Caserta, Italy

[3] Institute of Geophysics, Polish Academy of Sciences, ul. Księcia Janusza 64, 01-452 Warsaw, Poland

## 1 Introduction

Subglacial lakes are a peculiar important component of the basal hydrological system of the Antarctic ice sheet, about 400 in number; in Arctic, just four subglacial lakes have been, so far, clearly identified by airborne radio-echo sounding in Greenland (Palmer et al. 2013; Howat et al. 2015; Willis 2015). Isolated (*not* interconnected) subglacial

lakes result a possible source of information tracing back to past geological periods, being such their life length. In those cases, any local inspection by deep drilling operation must be conducted with extreme care to avoid water spoiling and preserve the physical, chemical, and (presumably) biological equilibria. Studies based on mathematical modeling and numerical simulation are, clearly, encouraged. It is worth to remind that from the study of the subglacial hydrological network in the polar regions, lakes included, hints might be extrapolated also on the characteristics of the sub-surface ocean conjectured underneath the icy crust of several satellites of the solar system (Carr et al. 1998; Mitri and Showman 2005) (e.g., Europa and Enceladus, respectively, Jupiter's and Saturn's satellites), possibly revealing extra-terrestrial environments potentially suitable for life.

This work deals with a numerical algorithm for the assessment of the conjecture of a subglacial lake, tested on a likely basin underneath Amundsenisen Plateau at South-Spitzbergen, Svalbard. The interest of this investigation is increased by the fact that deposits from the period before glaciation of Europe and Scandinavia might have gathered in such a basin, and also this one might be just the first to be localized there.

The structure of the paper is the following: Sect. 2 deals with the geographical and physical description of the test problem; in Sect. 3, adopted simplifying assumptions are presented and discussed; in Sect. 4, the numerical algorithm is described and, in Sect. 5, conclusions are drawn on the response of the algorithm versus the conjecture assessment via representative numerical results.

## 2 Conjecture set-up

Ground-based radio-echo sounding records of the Amundsenisen Plateau have revealed several 'flat' bed sections, the largest one being 450 m long (Glowacki et al. 2007). Amundsenisen Plateau is an accumulation icefield, 80 $km^2$ in area, with the thickest firn-ice cover of the archipelago (631 m maximum thickness), occupying a large depression surrounded by mountain ridges, controlled by geological structure, with three outlet channels. It spreads from 77°13′N to 77°20′N and from 15°6′E to 15°44′E.

From thermal viewpoint, this one is a temperate icefield, that is, except for the upper layer of snow and firn, it consists of ice at melting temperature. By reflecting properties and estimates of the hydraulic potential field, the 'flat' bed sections might be interpreted as from near-bottom water bodies, indeed, very similar to radar reflection from subglacial lakes, although they might also be the sign of water film on flat bedrock areas.

In the upper left part of Fig. 1, the top surface of Amundsenisen Plateau is plotted with the record of the ice velocity measured at upper reaches of Högsterbreen, Böygisen, and Paierlbreen, the outlet glaciers: the values are 7.22, 10.65, and 9.30 cm/day, respectively (Glowacki et al. 2008). The lower right part of the same figure shows the top surface ice velocity field, as it results (Mansutti et al. 2015) by ignoring the lake and running the 3D ELMER/ICE code up to regime on the geometrical domain occupied by Amundsenisen Plateau (open source http://www.csc.fi/elmer/, only ice dynamics and thermodynamics, refer to Gagliardini et al. 2013). The dark-green ice flow-lines end, respectively, to the three outlet glaciers. The ground-based radio-echo sounding flat signal spots are highlighted in light green; we have focussed on the largest one, located around (77°17′N, 15°25′E), and overtopped by the ice flowing to Högsterbreen. It is worth to stress that an ice-divide is visible between the considered flow and the central branch. The fact that the flat signal spots are placed beneath a flowing ice stream and in the proximity of an ice-divide, where water drainage occurs, is in support to the conjecture of the existence of corresponding subglacial lakes (Ridley et al. 1993). The locations of the focussed lake in the two drawings are connected with a light-blue arrowed line.

## 3 Simplifying assumptions

The proposed algorithm is linked to some environmental aspects that have inspired important simplifications of the modeling. Here, we summarize these items.

(1) *The spatial structure of the problem can be assumed two-dimensional*—this aspect is derived from the fact that, in the preliminary numerical simulation above mentioned that was developed on the real bedrock, ice flow above the considered conjectured lake is parallel rectilinear. In the present case, such a structure should persist also when the presence of the lake is included, because of its length (the measure of the lake surface diameter parallel to the ice flow)—about 460 m—being of the same order of Amundsenisen icefield thickness (Glowacki et al. 2007)—from 420 to 631 m. Mansutti et al. (2015) have already discussed this point, by contrast to arguments that Kwok et al. (2000) introduced for the case of Vostok lake (Antarctica), and inferred that, for its relatively *small* extension, conjectured lake cannot influence the overall sliding behaviour of the overlying icefield and, much less, impress a three-dimensional deviation to a rectilinear parallel ice flow. On the contrary, ERS1-SAR images of the area around Vostok lake exhibit curvy ice flow-lines, effect of the sliding velocity increase upon the subglacial lake surface followed by abrupt containing effect of the

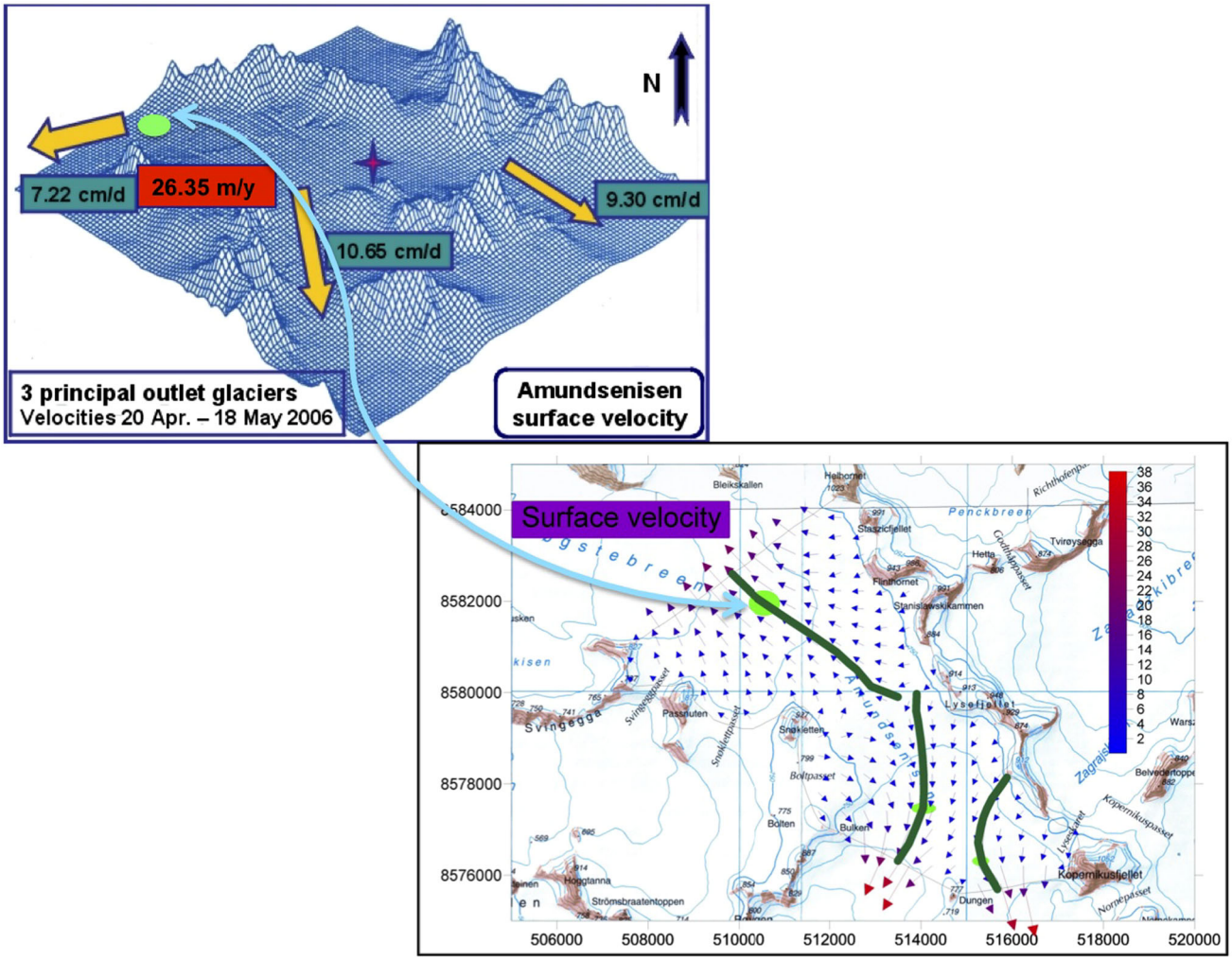



**Fig. 1** Amundsenisen Plateau (Svalbard): external surface with measured top surface ice velocity values at outlets (from Glowacki et al. 2008) (*above*) and simulated top surface ice flow field with light-green ovals in correspondence of ground-based radio-echo sounding flat signal spots (from Mansutti et al. 2015) (*below*)

downhill rocky bottom. However, Vostok lake maximum diameter measures 45 km that is ten times the ice cover thickness in Antarctica.

We have developed the numerical simulation on the two-dimensional vertical section parallel to the ice flow-lines where the driving force of the icefield on the lake water is maximum. Actually, supposing that, for the sake of simplicity, the conjectured lake has the shape of a spherical cap, in any other vertical two-dimensional section of the lake, as the buoyancy force supported by the geothermal heat amounts essentially the same, the composition of both forces—ice driven and buoyancy—ends in a system that is weaker than the corresponding one in the simulated section.

In any case, we can expect that a more realistic three-dimensional numerical simulation of the conjectured sub-glacial lake might end in a slower flow field, with the extension of the evolution time of the overall process but, presumably, without changes in the conclusions of the investigation.

(2) *Time change of the icefield top surface elevation can be neglected*—several factors contribute to the change of a grounded icefield top surface elevation, most important are the accumulation/ablation of snow on top (with the formation of a firn layer for successive melting and regelation local events), melting at the bottom of the icefield with water drainage through the soil and ice surge occurrences. The mathematical modeling of these aspects is closely linked to environmental data either only episodically available, as it is for the snow fall time series, or technically difficult to collect, as it is for the porosity of the soil, the local value of the geothermal heat flux, and the periodicity of ice surges. However, in the case of Amundsenisen Plateau, the laser altimetry data collected by J. Jania, L. Kolondra, and P. Glowacki show top surface elevation profiles essentially stationary during the time

span 1990–2005: Figs. 2 and 3 show the top surface elevation along the profile of interest, Hogsterbreen–Amundsenisen–Nornebreen, and the related annual average elevation change, respectively. It is noticeable that when at north-side Amundsenisen, (Hogsterbreen) a decrease was captured, an increase of comparable entity corresponded at south-side of it (Nornebreen), so that the spatial average of the elevation change at Amundsenisen is, indeed, quite small and may be considered negligible. In addition, Nuth et al. (2010) pointed out that observation data on the long-term (over the past 40 years) confirm this trend. This means that the overall effect of snow accumulation/ablation on top surface, water drainage through the bottom rocks, and surge occurrences, in terms of ice mass balance, is negligible during this time span. We have assumed this peculiarity as permanent and, then, ignored such processes within mathematical modeling; moreover, we have fixed the icefield top surface at the observed position (equilibrium of the air/ice front) and imposed a Weertman-type sliding condition to the ice facing the rocky bottom (effect of the residual water film).

(3) *The impact of the temporal changes of air temperature and snow/firn layer temperature on the system can be neglected*—for the check of the likelihood of the existence of a subglacial lake, direct impact aspects within the system air/icefield/bedrock, either for thermo-dynamical effects and mechanical ones, are the known peculiar temperate state of the icefield above the conjectured lake and the geothermal heat flux from the rocky cavity where it would be hosted, that are experimental data. In such a context, we deduce that the snow and firn layer, typically 25 m thick on top of the temperate ice core (Paterson 2006), must have an insulating effect on the ice underneath so to guarantee that its temperature keeps at melting point: alike a sort of thick interface between air and the icefield core, it undergoes the effect of the external harsh temperature and its seasonal changes, damping the impact on the ice. Conversely, no drawback should come in maintaining, as we have fixed, the external temperature and the snow/-firn temperature profile constant in time, fixed at known values, collected from the literature and from a meteorological database as it follow. From field data on Amundsenisen icefield reported by Zagorodnov (1985), we have acquired the 17 m in-depth temperature vertical profile along the firn layer. Then, we have estimated the temperature vertical profile of the 8 m-thick snow layer covering firn by interpolating the top firn value and the annual average temperature at Amundsenisen Plateau, estimated from the temperature of the Hornsund meteorological station (a.s.l.), http://www.yr.no/sted/Norge/Svalbard/Svalbard_lufthavn_m%C3%A5lestasjon/varsel.rss—the closest one to the tested place available—with altitude correction (in that area amounting to −1 °C per 100 m added altitude). In Fig. 4, the resulting plot is sketched.

## 4 Numerical algorithm

The leading idea, here, has been to check if the inclusion of a subglacial lake underneath the icefield within our numerical simulation yields results compatible with the available measured data. At this purpose, with the

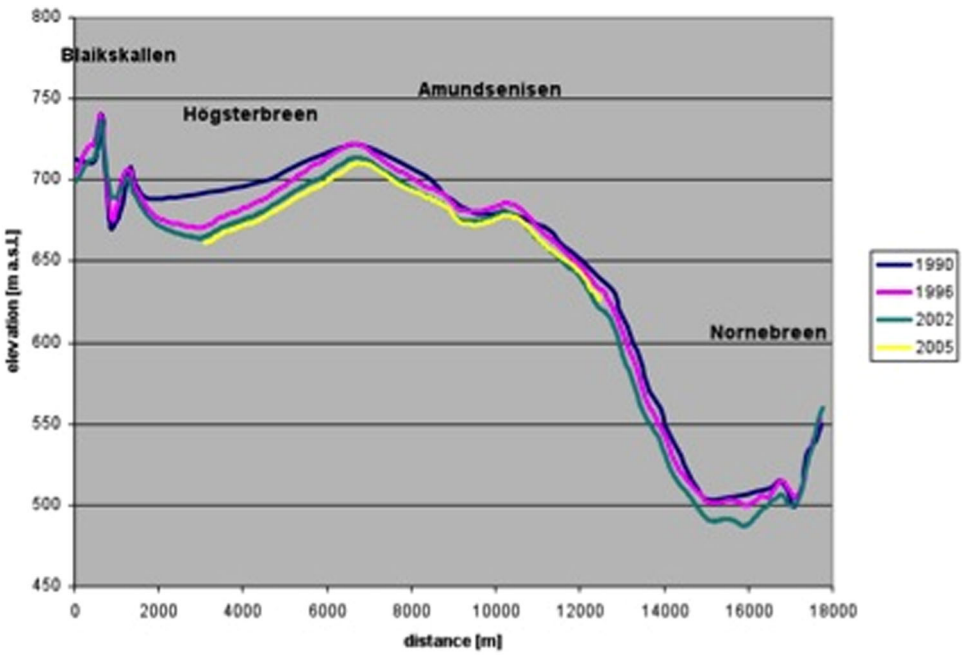



**Fig. 2** Top surface elevation along the icefield profile Hogsterbreen–Amundsenisen–Nornebreen registered at several years (unpublished laser altimetry data and picture by J. Jania and L. Kolondra, (University of Silesia) and P. Glowacki, (Polish Academy of Science))

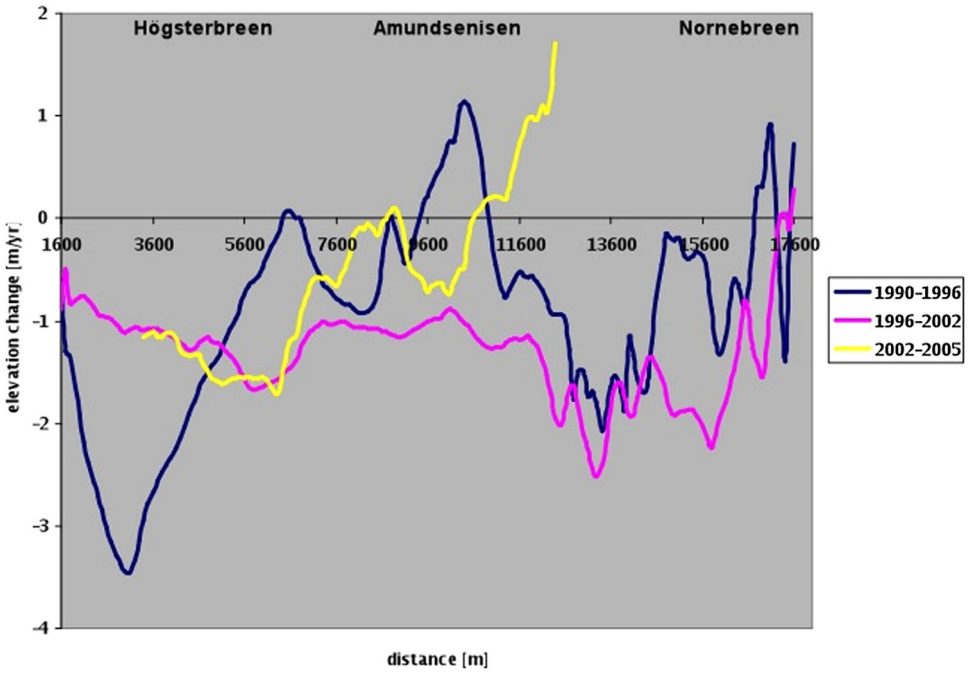



**Fig. 3** Annual average elevation change along the icefield profile Hogsterbreen–Amundsenisen–Nornebreen at several successive year intervals (unpublished laser altimetry data and picture by J. Jania and L. Kolondra (University of Silesia) and P. Glowacki (Polish Academy of Science))

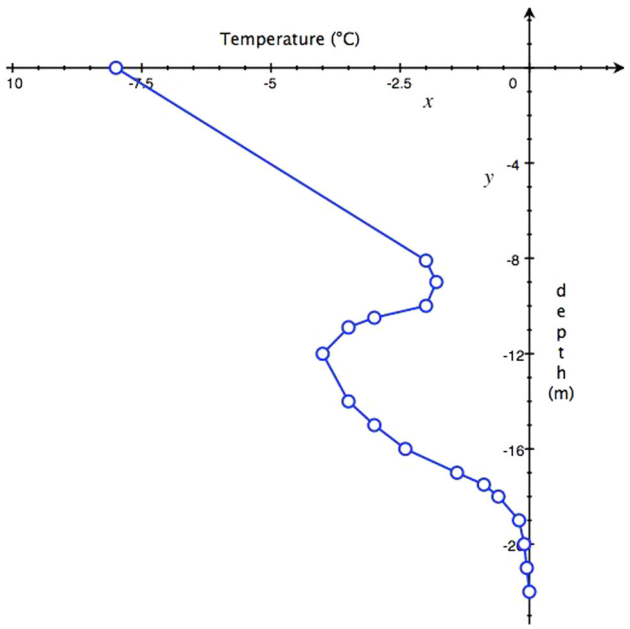



**Fig. 4** In-depth temperature profile of the snow/firn layer at Amundsenisen Plateau reconstructed by combining the field data by Zagorodnov (1985) and the annual average temperature at Hornsund as from records of the meteorological station (with correction by altitude)

assumptions above, we have studied the time evolution of the dynamics and thermodynamics of the icefield and of the subglacial lake within a fixed two-dimensional vertical rectangular section along the upper dark-green flow-line in Fig. 1, with a vertical side in correspondence of the ice-divide (see description in Sect. 2) and the opposite one placed at the beginning of Högsterbreen, outlet glacier. Bedrock topography, and top surface of the glacier respond to real data appeared in Glowacki et al. 2007 and Glowacki et al. 2008. As there is no hint about the real existence of a cavity in the bedrock hosting the subglacial lake, after a numerical sensitivity study on its necessary minimal depth, we had to fix a hypothetic basin (Mansutti et al. 2015).

The numerical algorithm, which we have built up, is based on a mathematical numerical model whose details have been presented and justified in Mansutti et al. (2015) and Mansutti et al. (2016). Here, we do not provide neither the equations nor their discretized form, but we only recall, in the following points, the main elements and, then, focus on the structure of the algorithm.

(a) Dynamics and thermodynamics of ice:

- the icefield is at melting temperature that is assumed as function of the pressure field, $T_m(p)$, according to Clausius–Clapeyron law;
- for rheology, Glen's law for temperate ice with $n = 3$, accounting for tertiary creep (Paterson 2006), is adopted. Except in snow and firn layer, ice water content is computed as solution of a transport equation with source term for water released via general strain heating (Hutter 1982, 1993; Greve 1995). In the upper layer, where only sliding motion occurs, correlation functions obtained for a similar glacier (Breuer et al. 2006) provide estimates of ice water content in terms of measured temperature values. Intergranular drainage is neglected, as permeability of temperate ice is, indeed, extremely low (Paterson 2006). We solve the unsteady

Stokes formulation of the dynamics equations with incompressibility constrain;

- a Weertman-type sliding condition is imposed for the motion of the icefield on the bedrock where a water film forms. As justified in Sect. 3, point (1), same sliding condition is imposed also above conjectured lake surface. Parameter calibration has been developed to match with the measured top surface ice velocity at the outlet.

(b) Dynamics and thermodynamics of the subglacial lake:

- Large Eddy Simulation (LES) formulation of the unsteady non-isothermal hydrodynamics equations with constant eddy viscosity and eddy diffusion coefficients is adopted. As water is quasi-thermal-incompressible (Gouin and Ruggeri 2012), buoyancy force is included with Chen and Millero's (1986) density function (equation of state). After choosing a spatial mesh, the calibration of the eddy coefficients has been accomplished by meeting the order of magnitude of the velocity field of other subglacial lakes (e.g. Vostok lake);
- the estimate of the geothermal heat flux, $q_{\mathrm{geo}} = 37.5$ - mW/m$^2$, is taken from literature referring to similar environment.

(c) Ice/water phase-change process:

- at the phase front, in line with the related conservation laws, the continuity of momentum, mass, and energy is imposed via the so-called jump conditions. The phase-change mechanism, as release/absorption of latent heat, contributes to the energy balance and provides the local value of the progression velocity of the icefield/subglacial lake front.

(d) The equations resulting from (a) to (c) are coupled:

- they are completed with boundary conditions corresponding to the natural set-up so to form a closed partial differential system. This one is solved via a second-order space and time finite volume discretization method and with a linearization technique, which preserves good coupling among the equations. At each time step and for each phase, a linear system is solved and the updated value of processed variables is promptly introduced in next step. At each time, iteration phase front is re-drawn, according to the output from energy jump condition, space mesh in both phase domains is adjusted, and related discretized variable values are re-computed via linear interpolation on the new points (extrapolation might be required only at phase front).

The computational algorithm can be summarized with the pattern illustrated in Fig. 5: the sketched time cycle includes the computational procedure for one-time-step numerical integration of the equations for the subglacial water (package I), for the icefield (package II) and for the ice/water interface (package III); package IV re-computes the space mesh of the updated icefield/lake domain. As water time scale is much smaller than ice time scale, we have obtained a significant cutoff of the computing time by advancing in time solely water solution—with a proper fractional time step—up to reach a cumulative time step suitable for ice, when package II and package III are run to update ice variables and ice/water front position.

In this context, we show that a lower limit of time step for the integration of ice and subglacial water differential equations, called $\Delta t_{\mathrm{i}}^{\mathrm{min}}$ and $\Delta t_{\mathrm{w}}^{\mathrm{min}}$, differs approximately of three orders of magnitude. This result is obtained considering the order of magnitude of the estimate of the

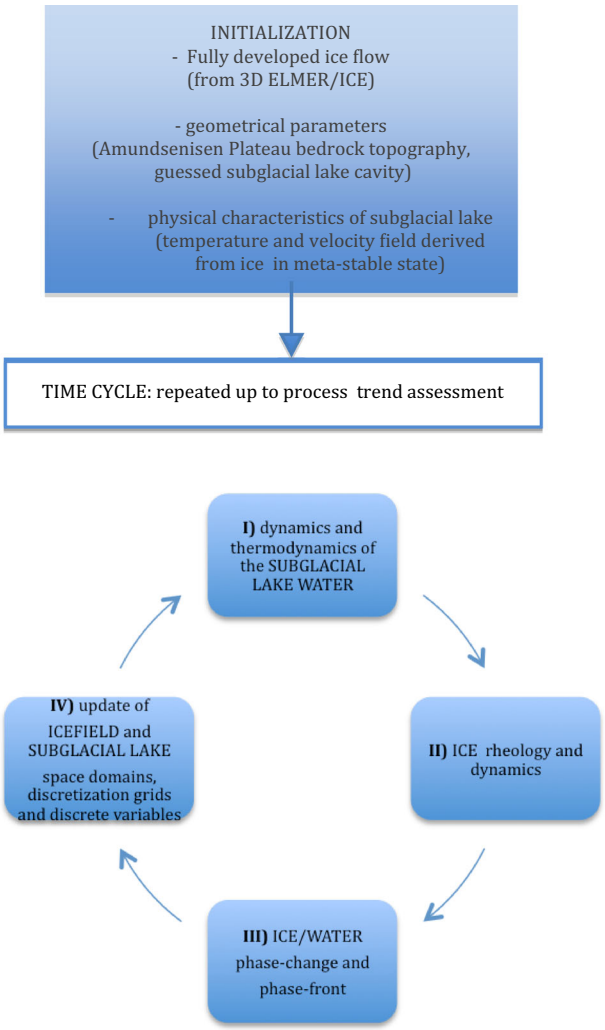



**Fig. 5** Plan of the computational algorithm

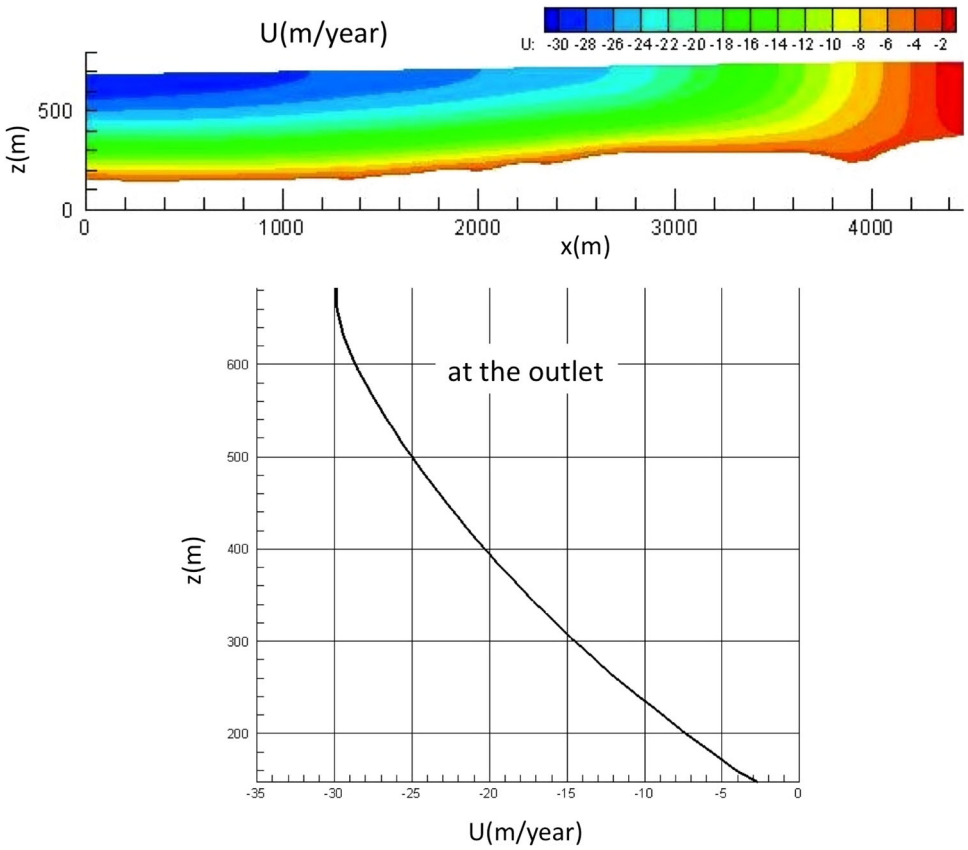



**Fig. 6** Ice horizontal velocity at steady regime, $t = 20{,}000$ days: iso-surfaces (*top*) and vertical profile at the outlet

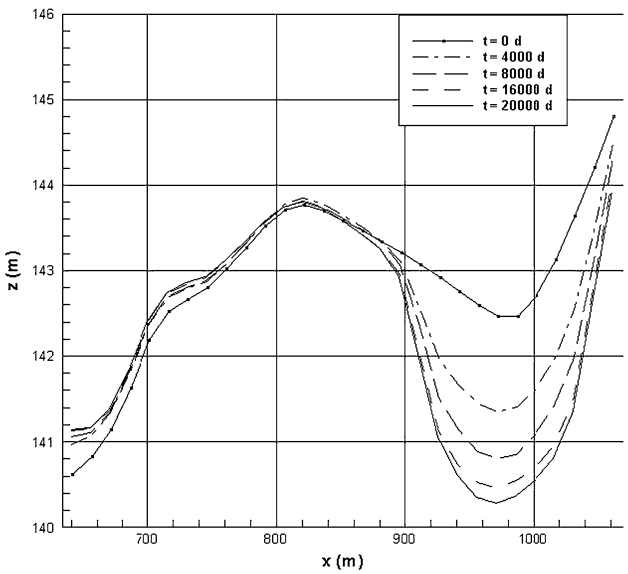



**Fig. 7** Time evolution of the icefield/subglacial lake interface

maximum value of ice and subglacial water velocity fields, respectively, $O(u_{\mathrm{i}}^{\max})$ and $O(u_{\mathrm{w}}^{\max})$, and the minimum step of the adopted finite volume discretization mesh of the two phases equations, respectively, $\Delta s_{\mathrm{i}}^{\min}$ and $\Delta s_{\mathrm{w}}^{\min}$:

$$\Delta t_{\mathrm{i}}^{\min} = \frac{\Delta s_{\mathrm{i}}^{\min}}{O(u_{\mathrm{i}}^{\max})} = \frac{2\,\mathrm{m}}{8.23 \times 10^{-7}\,\mathrm{m/s}} = 2.4 \times 10^{6}\,\mathrm{s},$$

$$\Delta t_{\mathrm{w}}^{\min} = \frac{\Delta s_{\mathrm{w}}^{\min}}{O(u_{\mathrm{w}}^{\max})} = \frac{1\,\mathrm{m}}{10^{-3}\,\mathrm{m/s}} = 10^{3}\,\mathrm{s}.$$

The above implies that, within the chosen space resolution for the numerical solution of the two phases equations, to capture a change in time of the magnitude of the ice velocity field, it is required a time step amounting at least to $\Delta t_{\mathrm{i}}^{\min} \approx 10^3 \cdot \Delta t_{\mathrm{w}}^{\min}$, that is $10^3$ times the time step suitable to capture a change in time of the magnitude of the water velocity and temperature fields.

With the above considerations, we obtain a safe of computing time equivalent to $10^3$ times the computing time of one time step for the ice phase.

Another important aspect for the choice of the time step is numerical stability imposing upper limitations that we have managed by trial and error.

## 5 Numerical results: conclusions

As benchmark quantities for the numerical simulation, we have adopted the measured value of the top surface ice velocity at the outlet glacier (Högsterbreen) that amounts to

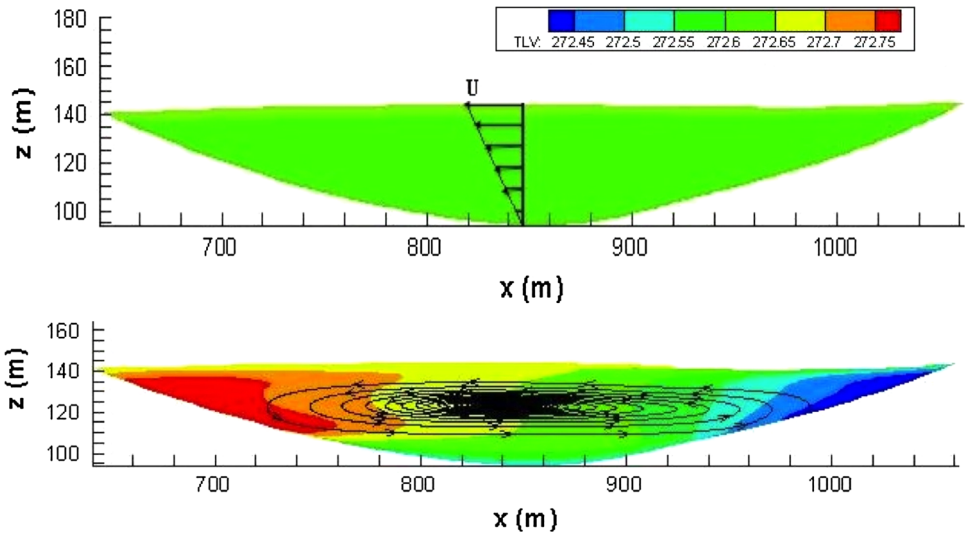



**Fig. 8** Subglacial lake: temperature distribution and horizontal velocity along the vertical midline at $t = 0$ day (*top*) and temperature iso-surfaces with particle tracks at $t = 20{,}000$ days (*bottom*)

26.35 m/year (see Fig. 1), and the interface profile between the supposed subglacial lake and the icefield which is known by ground penetrating radar (GPR) measurements. Prior to comparison, it is worth to remind that the measured surface ice velocity value is subject to an intrinsic error, as it results from a local (in space and time) measurement operation. About the second target, it is known that GPR measurements undergo a systematic error of $\pm 3.5$ m.

From the initial time $t = 0$ day, we have pushed forward the numerical simulation up to time $t = 20{,}000$ days, when the ongoing process has clearly revealed its trend.

In Fig. 6, we plot the computed ice horizontal velocity iso-surfaces and related vertical profile at the outlet at time $t = 20{,}000$ days; a subglacial lake is conjectured in the abscissa subinterval [640, 1,060] (it is not drawn here). It is apparent that the numerical top surface velocity at the outlet reaches the value 30 m/year that is affected by 14 % relative error versus measured value. Ice initial flow was assigned equal to the preliminary simulation result computed with 3D ELMER/ICE, partially shown in Fig. 1 (bottom).

In Fig. 7, a time sequence of numerical icefield/subglacial lake interfaces is shown. The initial profile was assigned equal to that one acquired from the GPR survey; it can be seen that, as the simulated time goes on, the lake front converges within a range certainly covered by the typical GPR measurement error. This implies that, within set conditions and time $t = 20{,}000$ days, the inclusion of a subglacial lake in the numerical simulation leads to results in agreement with measured datum. Now, let us examine how flow and temperature fields of ice evolve in the cavity of the conjectured lake. Figure 8 (top) shows the temperature iso-surfaces and the vector plot of the horizontal velocity along the vertical mid line at the initial time when it is supposed that the temperature of the ice placed there has reached values just slightly over melting point and, being still similar for rheology and dynamical behaviour, flows together with the ice of the overlain icefield. Figure 8 (bottom) shows the temperature iso-surfaces and the particle tracks in the basin cavity at final simulated time: it is clearly visible that a definite increase of temperature confirms the progress of the ice/water phase change, and also the onset of a weakly asymmetric recirculation driven by the icefield motion and enforced by the geothermal heat flux. A time sequence of temperature vertical profiles at $x = 720$ m, core of the formed water cavity, is shown in Fig. 9: from the plotted initial profile, one can derive the imperceptible perturbation artificially imposed to the temperature of the temperate ice to start the phase-change process (let us observe that $T = 272.66$ K is the value of melting temperature at the ice/water front). As a weak convection sets in, heat is transported by convection and diffusion and collects into the cavity leading to a progressive increase of temperature that leads temperate ice in the cavity to overcome metastability, definitely changing into water. The temperature profiles in Fig. 9 support this interpretation.

The assessment of the trend of the overall process is provided by Fig. 10 where we have reported a time sequence of metastability lines, separating the newly formed water from the metastable ice: we notice that such a curve moves forward, that is the size of the cavity occupied by water grows in time due to ongoing melting.

Within set conditions (see Sect. 3), including the occurrence of an initial increase of the temperature of the ice in the basin cavity starting the phase-change process, we can conclude that numerical simulation results are compatible with the formation of a subglacial lake and

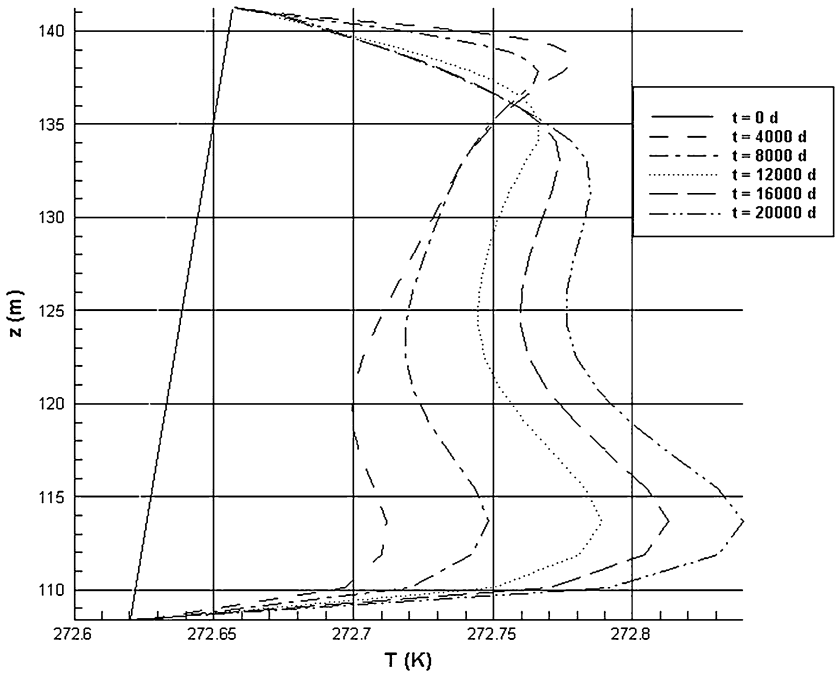



**Fig. 9** Subglacial lake: time sequence of temperature profiles along vertical midline of formed subglacial water cavity ($x = 720$ m)

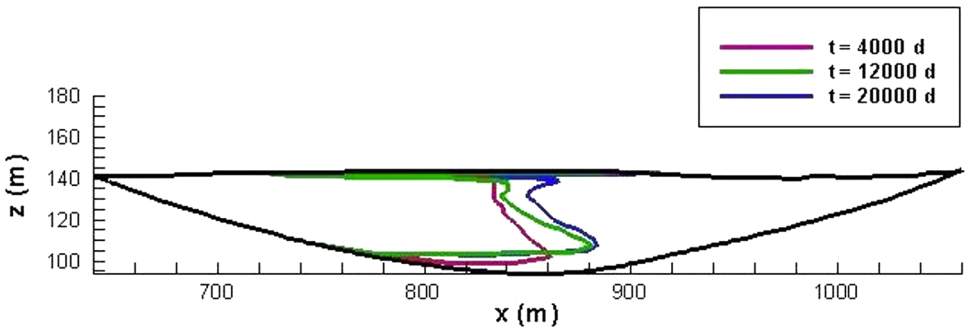



**Fig. 10** Subglacial lake formation: time progression of the metastability line attesting the increase of the molten ice mass

support the decision to undertake on-field investigations for further characterization.

**Acknowledgments** The authors acknowledge the ESF-ERANET Polar Climate Consortium for funding the transnational project SvalGlac—Sensitivity of Svalbard Glaciers to Climate Change (2010–2013); presented results are part of its accomplishments. In particular, the national agencies supporting the authors are the following: Piano Nazionale Ricerca Antartide (PNRA) (Mansutti) and Narodowe Centrum Badań i Rozwoju National (NCBiR) (Glowacki). Moreover, Mansutti wants to thank Prof. J. Jania (University of Silesia) and Prof. L. Kolondra (University of Silesia) for allowing the use of the pictures in Figs. 2 and 3 co-authored by them, and Prof. F. J. Navarro (Universidad Politecnica de Madrid) for his expert advice on glaciological issues.

## References

Breuer B, Lange MA, Blindow N (2006) Sensitivity studies on model modifications to assess the dynamics of a temperate ice cap, such as that on King George Island, Antarctica. J Glaciol 52(177):235–247

Carr MH, Belton MJS, Chapman CR, Davies ME, Geissler P, Greenberg R, McEwen AS, Tufts BR, Greeley R, Sullivan R, Head JW, Pappalardo RT, Klaasen KP, Johnson TV, Kaufman J, Senske D, Moore J, Neukum G, Schubert G, Burns JA, Thomas P, Veverka J (1998) Evidence for a subsurface ocean on Europa. Nature 391:363–365

Chen CT, Millero FJ (1986) Precise thermodynamic properties for natural waters covering only the limnological range. Limnol Oceanogr 31(3):657–662

Gagliardini O et al (2013) Capabilities and performance of Elmer/Ice, a new-generation ice sheet model. Geosci Model Dev 6:1299–1318. doi:10.5194/gmd-6-1299-2013

Glowacki P, Vasilenko EB, Macheret Y, Glazovsky AF, Moore J, Hagen JO, Navarro FJ (2007) Structure of Amundsenisen, Spitzbergen, from ground based radio echo sounding. In: Oerlemans J, Tijm-Reijmer CH (eds) The dynamics and mass budget of arctic glaciers, pp 43–44

Glowacki P, Vasilenko EB, Glazovsky AF, Macheret Y, Navarro FJ, Moore J, Hagen JO (2008) Stroyenye i gidrotermicheskaya struktura lednikovo plato Amundsena na Szpitsbergenye po dannym nazyemnogo radiozondirowanya. Materiały Glacjołogicheskich Issledovanij 105:97–104

Gouin H, Ruggeri T (2012) A consistent thermodynamical model of incompressible media as limit case of quasi-thermal-incompressible materials. Int J Non-linear Mech 47:688–693

Greve R (1995) Thermomechanisches Verhalten polythermer Eisschielde—Theorie, Analytik, Numerik. Phd thesis, Technische Hochschule, Darmstadt

Howat IM, Porter C, Noh MJ, Smith BE, Jeong S (2015) Brief communication: Sudden drainage of a subglacial lake beneath the Greenland Ice Sheet. Cryosphere 9:103–108. doi:10.5194/tc-9-103-2015

Hutter K (1982) Dynamics of glaciers and large ice masses. Annu Rev Fluid Mech 14:87–130

Hutter K (1993) Thermo-mechanically coupled ice-sheet response—cold, polythermal, temperate. J Glaciol 39(131):65–86

Kwok R, Siegert M, Carsey F (2000) Ice motion over Lake Vostok, Antarctica: constrains in inferences regarding the accreted ice. J Glaciol 46:689–694

Mansutti D, Bucchignani E, Otero J, Glowacki P (2015) Modelling and numerical sensitivity study on the conjecture of a subglacial lake at Amundsenisen, Svalbard. Appl Math Model 39:4266–4284. doi:10.1016/j.apm.2014.12.043

Mansutti D, Bucchignani E, Glowacki P (2016) Numerical validation of the conjecture of a subglacial lake at Amundsenisen, Svalbard. Appl Math Model. doi:10.1016/j.apm.2016.03.030

Mitri G, Showman AP (2005) Convective–conductive transitions and sensitivity of a convecting ice shell to perturbations in heat flux and tidal-heating rate: implications for Europa. Icarus 177:447–460

Nuth C, Moholdt G, Kohler J, Hagen JO, Kääb A (2010) Svalbard glacier elevation changes and contribution to sea level rise. J Geophys Res 11:1–16

Palmer SJ, Dowdeswell JA, Christoffersen P, Young DA, Blankenship DD, Greenbaum JS, Benham T, Bamber J, Siegert M (2013) Greenland subglacial lakes detected by radar. Geophys Res Lett 40:6154–6159

Paterson WSB (2006) The physics of glaciers. Butterworth-Heinemann, Elsevier Science, UK

Ridley JK, Cudlip W, Laxton SW (1993) Identification of subglacial lakes using ERS-1 radar altimeter. J Glaciol 39:625–634

Willis MJ (2015) Re-charge of a subglacial lake by surface meltwater in north-east Greenland. Nature 518:223–227. doi:10.1038/nature14116

Zagorodnov VS (1985) Ldoobrazovanye i glubnoye stroyenie lednikov (Ice formation and inner structure of glaciers) (Russian). In: Kotlyakov VM (ed) Glyatsiologiya Spitsbergena. Nauka, Moskva, pp 119–147